

Asymptotic Bounds for the Traveling Salesman Problem with Drone

Jae Hyeok Lee^{*a}, Taekang Hwang^{†a}, and Changhyun Kwon^{‡a, b}

^aDepartment of Industrial and Systems Engineering, KAIST, Daejeon, 34141, Republic of Korea

^bOmelet, Inc., Daejeon, 34051, Republic of Korea

December 28, 2025

Abstract

The asymptotic behavior of the optimal TSP tour length is well known from the classical Beardwood–Halton–Hammersley theorem. We extend this result to the Traveling Salesman Problem with Drone (TSPD), a cooperative routing problem in which a truck and a drone jointly serve customers. Using a subadditive Euclidean functional framework, we establish the existence of an almost sure limit for the optimal TSPD makespan scaled by the square root of the problem size. We derive explicit upper and lower bounds for the speed-scaled Euclidean TSPD model: upper bounds are obtained via structured ring-based tour constructions and Monte Carlo evaluation, while lower bounds are derived from a parametric approach and known bounds on the Euclidean TSP constant. Computational results illustrate how tight the bounds are. We also derive and discuss lower bounds for the Rectilinear–Euclidean mixed TSPD model, in which truck travel is measured by the rectilinear distance and drone travel by the Euclidean distance.

Keywords: traveling salesman; unmanned aerial vehicles; probability; continuous approximation

1 Introduction

The seminal work of Beardwood, Halton and Hammersley (BHH 1959) showed that the length of the optimal TSP tour converges as the problem size increases. While the original result is more general, we focus on the case of the unit square in \mathbb{R}^2 .

Theorem 1 (BHH). Let X_1, X_2, \dots, X_n be a set of n points, uniformly distributed on the unit box $[0, 1]^2$, and let $\text{TSP}(\{X_1, X_2, \dots, X_n\})$ be the length of the optimal TSP tour. Then,

$$\lim_{n \rightarrow \infty} \frac{\text{TSP}(\{X_1, X_2, \dots, X_n\})}{\sqrt{n}} = \beta_{\text{TSP}} \quad (1)$$

for some positive constant β_{TSP} , almost surely.

*이재혁

†황태강

‡권창현; Corresponding author: chkwon@kaist.ac.kr

While the exact value of β_{TSP} is still unknown, empirical studies suggest that $\beta_{\text{TSP}} \approx 0.71$ (Johnson et al.; 1996; Choi and Schonfeld; 2022). Lower and upper bounds are known as follows:

$$0.6277 \leq \beta_{\text{TSP}} < 0.9038 \quad (2)$$

where the lower bound is by Gaudio and Jaillet (2020) and the upper bound is by Carlsson and Yu (2025).

The Beardwood–Halton–Hammersley (BHH) theorem has been widely used and extended in continuous approximation models in transportation (Daganzo; 1984a,b). Applications include location problems (Carlsson and Jones; 2022), the location-or-routing problem (Arslan; 2021), shared electric scooter rebalancing (Osorio et al.; 2021), bike-sharing market expansion (Fu et al.; 2022), and same-day delivery systems (Banerjee et al.; 2023). Readers are referred to the review articles by Langevin et al. (1996) and Ansari et al. (2018) for historical perspectives and a broader overview of applications.

In this paper, we aim to establish the existence of a BHH-type limit and derive explicit upper and lower bounds for a collaborative delivery problem known as the Traveling Salesman Problem with Drone (TSPD) defined in two-dimensional space (Murray and Chu; 2015; Agatz et al.; 2018). The TSPD utilizes a truck and a drone to fulfill the delivery needs, while allowing the drone to launch from and land on the truck. Establishing asymptotic bounds for TSPD is crucial for two reasons. First, it enables rapid, formula-based cost estimation for strategic logistics systems design as demonstrated in the continuous-approximation literature. Second, it provides a rigorous baseline for benchmarking large-scale heuristics, metaheuristics, or deep learning methods, where exact solutions are unattainable.

This study complements the work of Carlsson and Song (2018). They analyzed a coordinated truck-drone delivery problem, called the “horsefly” routing problem, in which the drone launches and rendezvouses with the truck at optimally chosen *continuous* points along the truck path. Asymptotic efficiency improvements of the coordinated delivery are studied via a continuous approximation model. In contrast, the TSPD restricts launching and landing to *discrete* points—the customer nodes. This discreteness introduces additional synchronization constraints while reflecting practical constraints imposed by the truck’s road network. Analyzing the characteristics of the connections among those discrete points, we establish a BHH-type asymptotic limit and derive lower and upper bounds for the coordinated delivery.

Our contributions are threefold. First, we prove the almost sure convergence of the TSPD makespan using a subadditive Euclidean functional framework. Second, we derive upper bounds by analyzing the properties of optimal TSPD solutions using a structured ring-based tour-construction framework. Most importantly, we prove that there always exists an optimal TSPD solution where the truck and drone never travel together. This structural property allows us to rule out many candidate configurations and substantially reduce the computational effort required to evaluate upper bounds. Third, to derive lower bounds, we devise a parametric approach that leverages known asymptotic properties of the Euclidean traveling salesman problem and nearest-neighbor distance distributions to bound the TSPD makespan as a function of the relative allocation of truck- and drone-served customers. Our parametric approach applies broadly to models in which the truck distance is measured by different metrics, such as the rectilinear and

Euclidean norms.

The rest of this paper is organized as follows. Section 2 summarizes the study on the TSP. Section 3 introduces the TSPD and proves the existence of the limit for the TSPD. Section 4 finds upper bounds, and Section 5 finds lower bounds. Section 6 demonstrates the bounds we found, Section 7 extends the result to the Rectilinear-Euclidean mixed model, and Section 8 concludes the paper.

2 Preliminaries

In this section, we provide a generalized result for the existence of the limit and summarize the approaches for bounding the limit in the TSP. These results will provide a basis for the TSPD analysis later.

2.1 The Existence of the Limit

Steele (1981) generalized the approach of Beardwood et al. (1959) for more general settings to prove the existence of the limit and provided an axiomatic approach. We consider a function $L : \mathbb{R}^{2n} \rightarrow \mathbb{R}$, which can represent the length of the optimal objective function of various combinatorial optimization problems, including TSP and TSPD.

Assumption 1. We make the following assumptions on the function $L(\cdot)$:

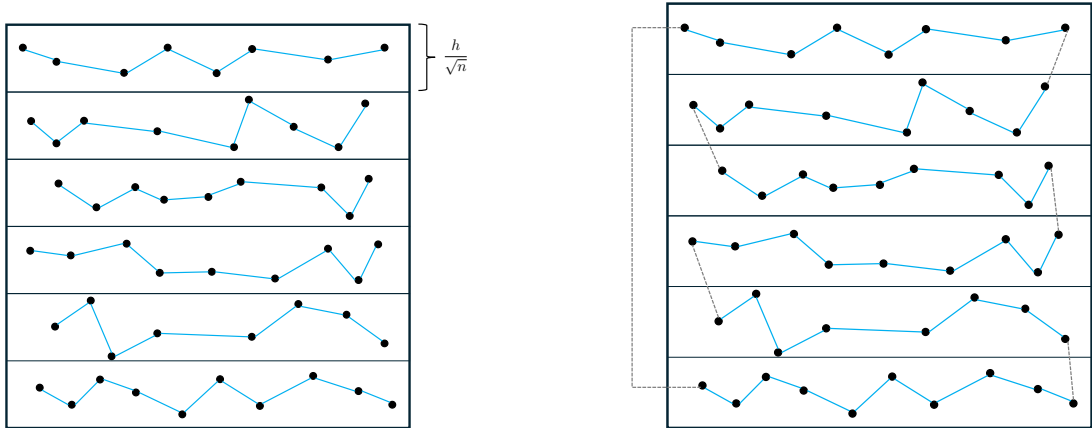
- (A1) *Positive Homogeneity.* $L(\{\lambda x_1, \dots, \lambda x_n\}) = \lambda L(\{x_1, \dots, x_n\})$ for all $\lambda > 0$.
- (A2) *Translational Invariance.* $L(\{x_1 + x, \dots, x_n + x\}) = L(\{x_1, \dots, x_n\})$ for any $x \in \mathbb{R}^2$.
- (A3) *Monotonicity.* $L(\{x\} \cup \mathcal{S}) \geq L(\mathcal{S})$ for any $x \in \mathbb{R}^2$ and finite subset $\mathcal{S} \subset \mathbb{R}^2$.
- (A4) *Finite Variance.* $\text{Var}(L(\{X_1, \dots, X_n\})) < \infty$ whenever X_1, \dots, X_n are independent and uniformly distributed on $[0, 1]^2$.
- (A5) *Subadditivity.* For any positive integer m , let $\{\mathcal{Q}_i : i = 1, 2, \dots, m^2\}$ be a partition of $[0, 1]^2$ into squares of length $1/m$. Let $\mathcal{X} = \{x_1, \dots, x_n\}$, and let $t\mathcal{Q}_i = \{tw : w \in \mathcal{Q}_i\}$ for any $t > 0$. There exists a constant $C > 0$ such that

$$L(\mathcal{X} \cap [0, t]^2) \leq \sum_{i=1}^{m^2} L(\mathcal{X} \cap t\mathcal{Q}_i) + Ctm.$$

Assumptions (A1) and (A2) indicate that the function $L(\cdot)$ is a Euclidean functional, of which TSP(\cdot) is a clear example. We note, however, that Euclidean functions from some combinatorial optimization problems are not monotone; for example, the minimum spanning tree problem. For such problems, we require an approach that involves smoothness (Rhee; 1993; Yukich; 2006).

The following theorem is a generalized result:

Theorem 2 (Steele 1981). Let X_1, X_2, \dots, X_n be a set of n points, uniformly distributed on the unit box $[0, 1]^2$. Suppose all conditions in Assumption 1 hold. There exists a constant $\beta(L)$



(a) Divide the unit square $[0,1]^2$ by strips with equal height of h/\sqrt{n} and connect points within each strip left to right.

(b) To complete a TSP tour, connect paths by extra lines, shown in dotted lines, whose total length is $o(\sqrt{n})$ almost surely.

Figure 1: Creating a feasible TSP tour that passes through n points in $[0,1]^2$. [Reproduced from Figure 1 of Carlsson and Yu (2025)]

such that

$$\lim_{n \rightarrow \infty} \frac{L(\{X_1, \dots, X_n\})}{\sqrt{n}} = \beta(L) \quad (3)$$

almost surely.

The subadditivity condition in (A5) is the most crucial part in guaranteeing the existence of the limit. Later, Yukich (2006) provided a simpler form of subadditivity:

(A5') *Geometric Subadditivity*. Let $\mathcal{X} = \{x_1, \dots, x_n\}$. If a rectangle \mathcal{Q} is divided into two rectangles \mathcal{Q}_1 and \mathcal{Q}_2 , there exists $C > 0$ such that

$$L(\mathcal{X} \cap \mathcal{Q}) \leq L(\mathcal{X} \cap \mathcal{Q}_1) + L(\mathcal{X} \cap \mathcal{Q}_2) + C \text{diam } \mathcal{Q}$$

where $\text{diam } \mathcal{Q}$ is the length of the diagonal of the rectangle \mathcal{Q} .

The geometric subadditivity (A5') implies (A5).

2.2 Poissonization

Consider n points, X_1, \dots, X_n , uniformly distributed in the unit box $[0,1]^2$. Due to the following lemma, we can focus on bounding the expected value instead of dealing with the 'almost surely' condition:

Lemma 1 (Beardwood et al. 1959).

$$\lim_{n \rightarrow \infty} \frac{\mathbb{E}[\text{TSP}(X_1, X_2, \dots, X_n)]}{\sqrt{n}} = \beta_{\text{TSP}}. \quad (4)$$

Further, we notice that considering n points in $[0,1]^2$ is the same as considering the Poisson process with intensity n (Beardwood et al.; 1959). Using this observation, we can find an upper bound on β_{TSP} .

Consider strips of the box with height h/\sqrt{n} for some constant $h > 0$, as shown in Figure 1. There are \sqrt{n}/h strips. In each strip, the number of points is $\frac{n}{\sqrt{n}/h} = h\sqrt{n}$ on average. Let $m = h\sqrt{n}$. In each strip, we will connect the points by straight lines in the order of their horizontal coordinates.

Consider the horizontal coordinates first. For any arbitrary interval of length δ , a point lies inside this interval with probability δ and outside with probability $1 - \delta$. Therefore, we can consider this as a Bernoulli trial. The number of points in this interval is distributed as Binomial(m, δ). When m is large and δ is small, it is well known that the Binomial distribution behaves like Poisson($m\delta$). Since intervals of length δ are independent of each other, we can now consider the entire interval $[0, 1]$ as a Poisson point process with intensity m .

This implies that the distance between two consecutive horizontal coordinates is distributed as Exponential(m). Let us denote the horizontal coordinate of point X_i by $X_i^{(1)}$. Considering two arbitrary consecutive points X_i and X_{i+1} , we have:

$$X_{i+1}^{(1)} - X_i^{(1)} \sim \text{Exponential}(h\sqrt{n}),$$

or, in the *unscaled* form,

$$Z \sim \text{Exponential}(1),$$

where $Z = h\sqrt{n}(X_{i+1}^{(1)} - X_i^{(1)})$.

Similarly, let us consider the vertical coordinates, denoted by $X_i^{(2)}$. In each strip of height h/\sqrt{n} , it is clear that $X_i^{(2)} = \frac{h}{\sqrt{n}}U$, where

$$U \sim \text{Uniform}([0, 1]).$$

2.3 Upper Bounds

Using these observations, we find an upper bound on β_{TSP} . First, we note that we do not need to consider the connections between the strips. Since there are \sqrt{n}/h number of strips, the total length of those connections is $o(\sqrt{n})$; therefore, it does not impact β .

For two arbitrary consecutive points $(X_i^{(1)}, X_i^{(2)})$ and $(X_{i+1}^{(1)}, X_{i+1}^{(2)})$:

$$\mathbb{E} \left\| \begin{pmatrix} X_{i+1}^{(1)} - X_i^{(1)} \\ X_{i+1}^{(2)} - X_i^{(2)} \end{pmatrix} \right\| = \mathbb{E} \left\| \begin{pmatrix} \frac{1}{h\sqrt{n}}Z \\ \frac{h}{\sqrt{n}}(U_1 - U_0) \end{pmatrix} \right\| = \frac{1}{h\sqrt{n}} \mathbb{E} \left\| \begin{pmatrix} Z \\ h^2(U_1 - U_0) \end{pmatrix} \right\|.$$

Recall that there are \sqrt{n}/h number of strips, and, in each strip, the number of points on average is $h\sqrt{n}$. Therefore, we obtain, for large n ,

$$\begin{aligned} \frac{\mathbb{E}[\text{TSP}(\{X_1, X_2, \dots, X_n\})]}{\sqrt{n}} &\leq \frac{1}{\sqrt{n}} \cdot \frac{\sqrt{n}}{h} \cdot (h\sqrt{n}) \cdot \frac{1}{h\sqrt{n}} \mathbb{E} \left\| \begin{pmatrix} Z \\ h^2(U_1 - U_0) \end{pmatrix} \right\| \\ &= \frac{1}{h} \mathbb{E} \left\| \begin{pmatrix} Z \\ h^2(U_1 - U_0) \end{pmatrix} \right\| \\ &= \frac{1}{h} \int_0^\infty \int_0^1 \int_0^1 e^{-z} \sqrt{z^2 + h^4(u-v)^2} \, dv \, du \, dz. \end{aligned}$$

We can write

$$\beta_{\text{TSP}} \leq \inf_{h>0} \frac{1}{h} \int_0^\infty \int_0^1 \int_0^1 e^{-z} \sqrt{z^2 + h^4(u-v)^2} \, dv \, du \, dz,$$

which is minimized near $h = \sqrt{3}$. The upper bound can be numerically evaluated to be 0.92116. Steinerberger (2015) later improved this bound as

$$\beta_{\text{TSP}} \leq 0.92116 - \frac{9}{16}10^{-6} \approx 0.9211594,$$

and Carlsson and Yu (2025) improved further as

$$\beta_{\text{TSP}} < 0.9038.$$

2.4 Lower Bounds

To find a lower bound, Beardwood et al. (1959) utilized the fact that each point is connected to two other points. If we assume that each point is connected to the nearest and the second-nearest points, then the total length of such connections will provide us with a lower bound. Of course, it may yield disconnected components, resulting in an infeasible solution. The approach is well described in Steinerberger (2015).

Lemma 2 (Steinerberger 2015). Let \mathcal{P}_n be a Poisson process on \mathbb{R}^2 with intensity n . Then, for any fixed point $p \in \mathbb{R}^2$, the probability distribution of the distance between p and the nearest point in \mathcal{P}_n is given by $f_1(r) = 2\pi n r e^{-\pi n r^2}$ and its expectation is $\frac{1}{2\sqrt{n}}$. The distance to the second-nearest point is distributed by $f_2(r) = 2\pi^2 n^2 r^3 e^{-\pi n r^2}$ and its expectation is $\frac{3}{4\sqrt{n}}$.

Consequently, Lemma 2 yields that

$$\text{TSP}(\{X_1, \dots, X_n\}) \geq \left(\frac{1}{2} + \frac{3}{4}\right) \frac{1}{\sqrt{n}} \frac{n}{2} = \frac{5}{8}\sqrt{n};$$

hence,

$$\beta_{\text{TSP}} \geq \frac{5}{8},$$

which was the result of Beardwood et al. (1959). Later Steinerberger (2015) and Gaudio and Jaillet (2020), respectively, improved the lower bound to

$$\beta_{\text{TSP}} \geq \frac{5}{8} + \frac{19}{10368} > 0.6268.$$

and

$$\beta_{\text{TSP}} \geq \frac{5}{8} + \frac{1}{2} \left(\frac{19}{10368} \right) + \frac{1}{2} \left(\frac{3072\sqrt{2} - 4325}{5376} \right) > 0.6277.$$

3 The TSPD Case

In this section, we first provide a formal definition of the TSPD and then show that the limit exists for the TSPD.

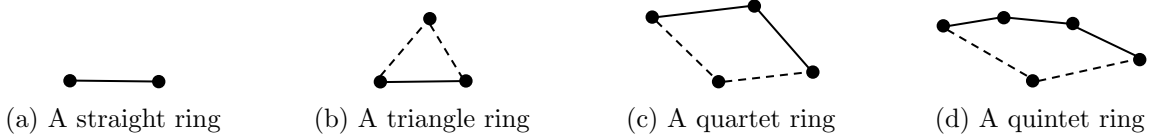


Figure 2: Rings. Solid lines are traveled by the truck, and dotted lines are traveled by the drone. In the straight ring, the truck travels with the drone attached.

3.1 The TSPD Defined

For any given set of points $\mathcal{X} = \{x_1, \dots, x_n\}$ with each $x_i \in \mathbb{R}^2$, the goal of the TSPD problem is to find coordinated truck and drone routes that minimize the total makespan of operations. We distinguish node types: *truck nodes* are visited only by the truck, *drone nodes* are served only by the drone, and *combined nodes* are synchronization points for both vehicles.

We adopt the term *rings* as the basic unit of TSPD solution constructions. Examples of rings are shown in Figure 4, and the definition of a ring is given below.

Definition 1. A *ring* is defined by two combined nodes serving as the start and end nodes, with at most one drone node and any number of truck nodes between them. For each ring r , the truck follows a path \mathcal{T}_r , and if a drone node is present, the drone follows a sortie path \mathcal{D}_r .

Let $\|\cdot\|_T$ denote the truck metric and $\|\cdot\|_D$ the drone metric—both norms defined in \mathbb{R}^2 . Define the truck and drone path costs as

$$t(\mathcal{T}_r) = \sum_{(i,j) \in \mathcal{T}_r} \|x_i - x_j\|_T, \quad d(\mathcal{D}_r) = \sum_{(i,j) \in \mathcal{D}_r} \|x_i - x_j\|_D.$$

The cost of a ring r is then:

$$\begin{aligned} c(r) &= c(\mathcal{X}_r) \\ &= \min_{\mathcal{T}_r, \mathcal{D}_r} c(\mathcal{T}_r, \mathcal{D}_r) \\ &= \min_{\mathcal{T}_r, \mathcal{D}_r} \begin{cases} \max\{t(\mathcal{T}_r), d(\mathcal{D}_r)\}, & \text{if } r \text{ contains a drone node,} \\ t(\mathcal{T}_r), & \text{otherwise,} \end{cases} \end{aligned}$$

where we abuse notation by defining \mathcal{X}_r as the set of points in ring r , with the first and last points being the two combined nodes.

A feasible solution to the TSPD problem is a set of rings $\mathcal{R}(\mathcal{X})$ that together cover all points in \mathcal{X} . The objective is to minimize the total cost:

$$\text{TSPD}(\mathcal{X}) = \min_{\mathcal{R}(\mathcal{X})} \sum_{r \in \mathcal{R}(\mathcal{X})} c(r),$$

which is the makespan.

3.2 The Existence of the Limit

We present the existence of the limit for the TSPD case.

Theorem 3. If X_1, \dots, X_n are independent and uniformly distributed in $[0, 1]^2$, then there exists a constant β_{TSPD} such that

$$\lim_{n \rightarrow \infty} \frac{\text{TSPD}(\{X_1, \dots, X_n\})}{\sqrt{n}} = \beta_{\text{TSPD}}, \quad (5)$$

almost surely.

Proof. We show that (A1)–(A4) and (A5') hold for $\text{TSPD}(\cdot)$.

(A1) *Positive Homogeneity.* Since norms are homogeneous, $t(\lambda\mathcal{T}_r) = \lambda t(\mathcal{T}_r)$ and $d(\lambda\mathcal{T}_r) = \lambda d(\mathcal{T}_r)$. Then, we can easily show that $c(\lambda\mathcal{X}_r) = \lambda c(\mathcal{X}_r)$; consequently, $\text{TSPD}(\lambda\mathcal{X}) = \lambda \text{TSPD}(\mathcal{X})$.

(A2) *Translational Invariance.* This clearly holds.

(A3) *Monotonicity.* This clearly holds.

(A4) *Finite Variance.* It is clear that

$$0 \leq \text{TSPD}(\{X_1, \dots, X_n\}) \leq \text{TSP}(\{X_1, \dots, X_n\}).$$

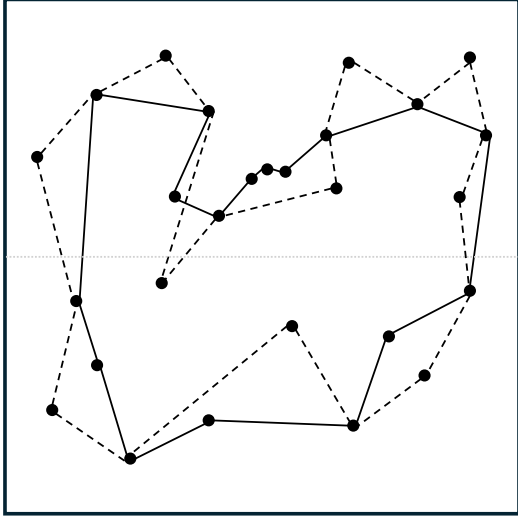
Since $\text{TSP}(X_1, \dots, X_n)$ is bounded from above, so is $\text{TSPD}(\{X_1, \dots, X_n\})$. We conclude that $\text{Var}(\text{TSPD}(\{X_1, \dots, X_n\}))$ is finite.

(A5') *Geometric Subadditivity.* Let \mathcal{Q} be a rectangle in \mathbb{R}^2 that is split into two rectangles with disjoint interiors, \mathcal{Q}_1 and \mathcal{Q}_2 , so that $\mathcal{Q} = \mathcal{Q}_1 \cup \mathcal{Q}_2$. For any finite point set $\mathcal{X} \subset \mathbb{R}^2$, define $\mathcal{X}_i := \mathcal{X} \cap \mathcal{Q}_i$. Assign points on the common boundary to either side arbitrarily so that $\mathcal{X} = \mathcal{X}_1 \cup \mathcal{X}_2$ and $\mathcal{X}_1 \cap \mathcal{X}_2 = \emptyset$. Let \mathcal{R} , \mathcal{R}_1 , and \mathcal{R}_2 be an optimal ring family for \mathcal{X} , \mathcal{X}_1 , and \mathcal{X}_2 , respectively. Figure 3a shows \mathcal{R} , and Figure 3b shows \mathcal{R}_1 and \mathcal{R}_2 .

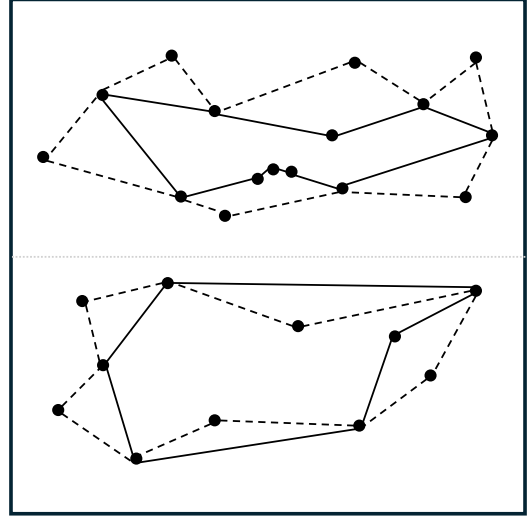
We illustrate the bounding procedure by the example shown in Figure 3. Choose arbitrary *combined* nodes $a \in \mathcal{X}_1$ and $b \in \mathcal{X}_2$, which will be used as endpoints. If a straight ring connects these endpoints, then remove the straight ring. If not, break any adjacent ring and choose the drone node as an endpoint. By introducing straight rings to connect the broken rings, we can construct a feasible TSPD solution for \mathcal{X} , which we denote by \mathcal{R}' . See Figure 3c for example.

We show that the $c(\mathcal{R}')$ can be bounded by the sum of $c(\mathcal{R}_1)$, $c(\mathcal{R}_2)$, and the length of the newly added straight rings as follows:

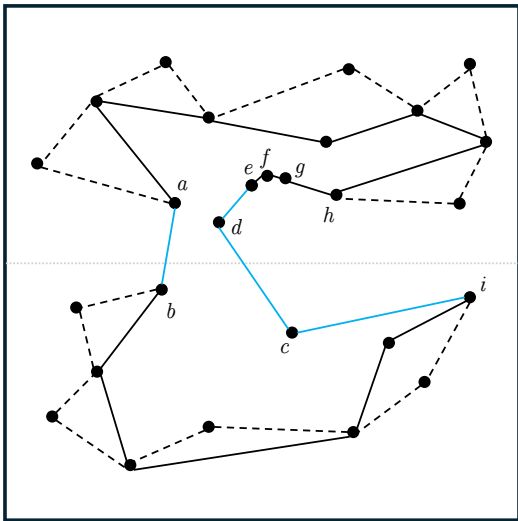
$$\begin{aligned} \text{TSPD}(\mathcal{X}) &= c(\mathcal{R}) \\ &\leq c(\mathcal{R}') \\ &= c(\mathcal{R}_1) + c(\mathcal{R}_2) + \|a - b\|_T + \|i - c\|_T + \|c - d\|_T + \|d - e\|_T \\ &\quad - \|a - e\|_T - \|b - i\|_T - \|a - d\|_D - \|d - h\|_D - \|b - c\|_D - \|c - i\|_D \\ &\leq c(\mathcal{R}_1) + c(\mathcal{R}_2) + \|a - b\|_T + \|i - c\|_T + \|c - d\|_T + \|d - e\|_T \\ &= \text{TSPD}(\mathcal{X}_1) + \text{TSPD}(\mathcal{X}_2) + \|a - b\|_T + \|i - c\|_T + \|c - d\|_T + \|d - e\|_T, \end{aligned}$$



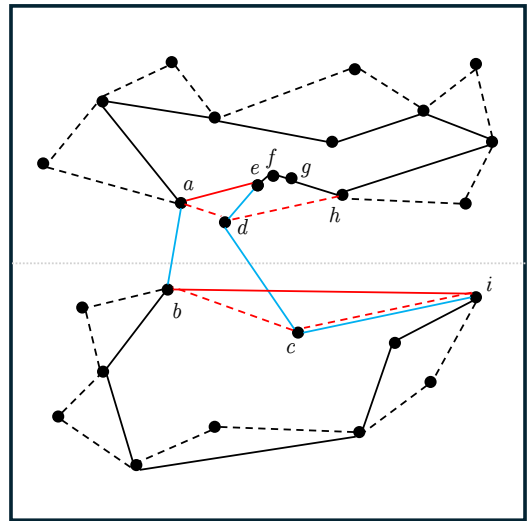
(a) An optimal TSPD solution for \mathcal{X} .



(b) Optimal TSPD solutions, \mathcal{R}_1 and \mathcal{R}_2 , for \mathcal{X}_1 and \mathcal{X}_2 .



(c) A constructed feasible TSPD solution for \mathcal{X} by breaking existing rings and adding new straight rings (shown in blue).



(d) Putting back removed connections (shown in red) from optimal solutions for \mathcal{X}_1 and \mathcal{X}_2 .

Figure 3: Comparison of optimal and constructed feasible solutions for $\mathcal{X} \cap \mathcal{Q}$.

which is illustrated in Figure 3d. Note that there are four additional terms in the last equality, and they are all measured in $\|\cdot\|_T$.

In general, there are no more than four additional terms if we remove rings on both \mathcal{R}_1 and \mathcal{R}_2 . This holds because we assumed that the drone may visit at most one customer node in a single flight.

Since all norms in \mathbb{R}^2 are equivalent, there exists $C_T > 0$ such that $\|p\|_T \leq C_T \|p\|_2$ for all $p \in \mathbb{R}^2$. Therefore, we conclude that

$$\text{TSPD}(\mathcal{X}) \leq \text{TSPD}(\mathcal{X}_1) + \text{TSPD}(\mathcal{X}_2) + 4C_T \text{diam}(\mathcal{Q}),$$

which is (A5') with $C = 4C_T$.

With (A1)–(A4) and (A5') holding, we have a proof of the theorem. \square

3.3 The Speed-Scaled Euclidean Model

If both truck and drone costs are based on the Euclidean norm, $\|\cdot\|_2$, and the drone operates at relative speed $\alpha \geq 1$, then

$$\|x_i - x_j\|_T = \|x_i - x_j\|_2, \quad \|x_i - x_j\|_D = \frac{1}{\alpha} \|x_i - x_j\|_2.$$

This model is commonly used in the literature (Agatz et al.; 2018; Boggyrbayeva et al.; 2023; Mahmoudinazlou and Kwon; 2024).

3.4 The Rectilinear-Euclidean Mixed Model

Several TSPD studies (Poikonen et al.; 2019; de Freitas and Penna; 2020) have considered the Rectilinear-Euclidean mixed norm case. That is, the truck's distance is measured by ℓ_1 -norm, while the drone's distance is measured by the speed-scaled ℓ_2 -norm. In particular,

$$\|x_i - x_j\|_T = \|x_i - x_j\|_1, \quad \|x_i - x_j\|_D = \frac{1}{\alpha} \|x_i - x_j\|_2,$$

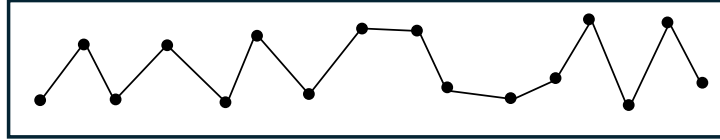
for the drone speed parameter $\alpha \geq 1$.

For the result of this paper, we consider this speed-scaled Euclidean model to derive bounds, while we make some comments on the Rectilinear-Euclidean mixed model in Section 7.

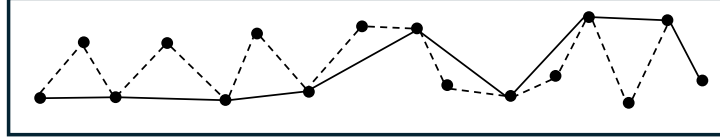
4 Upper Bounds

We consider the speed-scaled Euclidean distance model in Section 3.3. To derive an explicit upper bound for β_{TSPD} , we adapt the classical strip-partition method of Beardwood et al. (1959) to the TSPD setting. The key idea is to construct a feasible tour by tiling the plane with narrow strips and organizing customers into *rings* of simple structure.

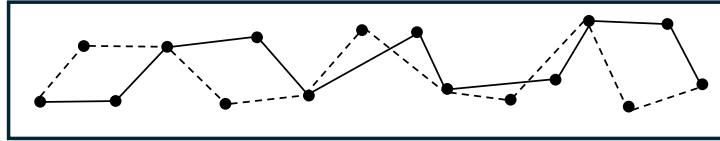
In the formation of a feasible TSPD route, we consider three primitive types: straight, triangle, and quartet rings. A *straight ring* consists of two combined nodes connected directly by the truck while the drone is on board; this is called a 2-point ring. A *triangle ring* consists of two



(a) Straight rings only



(b) Triangle rings only, with one “leftover” in the far right



(c) Quartet rings only

Figure 4: Three types of rings.

combined nodes with one drone node in between; this is a 3-point ring. A *quartet ring* consists of two combined nodes, one drone node, and one truck node; this is a 4-point ring. Similarly, a *quintet ring* consists of two combined nodes, one drone node, and two truck nodes; a 5-point ring. We will first form a feasible routing solution within each strip, only using homogeneous ring types; for example, a solution with straight rings only, triangle rings only, or quartet rings only.

Consider the set of arbitrary consecutive k points, X_0, X_1, \dots, X_{k-1} . We introduce unscaled random variables:

$$Z_1, Z_2, \dots, Z_{k-1} \stackrel{\text{i.i.d.}}{\sim} \text{Exponential}(1), \quad U_0, U_1, \dots, U_{k-1} \stackrel{\text{i.i.d.}}{\sim} \text{Uniform}[0, 1],$$

For each strip with height h/\sqrt{n} , we denote the unscaled cost of a k -point ring by $C_k(h, \alpha)$ for given h and the drone speed factor α . For example, the triangle ring is a 3-point ring with $k = 3$. For brevity, we will also use C_k to denote $C_k(h, \alpha)$ whenever the meaning is clear.

4.1 Straight Rings Only

Consider a straight ring, where the truck and the drone travel together at the speed of the truck. As seen in the TSP case, the unscaled distance between X_0 and X_1 can be written as:

$$L_{01} = \sqrt{Z_1^2 + h^4(U_0 - U_1)^2}.$$

This becomes the cost of the straight ring directly:

$$C_2 = L_{01}.$$

If we construct a TSPD path using straight rings only, as shown in Figure 4a, we can conclude that the limit is bounded by

$$\beta_{\text{TSPD}} \leq \frac{1}{h} \mathbb{E}[C_2] = \frac{1}{h} \int_0^\infty \int_0^1 \int_0^1 e^{-z_1} \sqrt{z_1^2 + h^4(u_0 - u_1)^2} du_0 du_1 dz_1.$$

4.2 Triangle Rings Only

We consider $\{X_0, X_1, X_2\}$ and the unscaled distances:

$$\begin{aligned} L_{01} &= \sqrt{Z_1^2 + h^4(U_0 - U_1)^2}, \\ L_{12} &= \sqrt{Z_2^2 + h^4(U_1 - U_2)^2}, \\ L_{02} &= \sqrt{(Z_1 + Z_2)^2 + h^4(U_0 - U_2)^2}. \end{aligned}$$

Forming triangle rings, we only consider the mid-point, X_1 , as the drone node. This is to ensure the connectivity and the independence between consecutive triangle rings. The cost of the triangle ring is

$$C_3 = \max \left\{ L_{02}, \frac{1}{\alpha} (L_{01} + L_{12}) \right\}$$

Note that each triangle ring consumes 2 additional points. Depending on the number of points within each strip, it is possible that we have a “leftover” node that cannot be part of a triangle ring, as shown in Figure 4b. We need to connect leftover nodes by a straight ring. However, such parts have a total length of $o(\sqrt{n})$, hence they do not impact β_{TSPD} . Using triangle-ring-only TSPD paths, we conclude that the limit is bounded by

$$\begin{aligned} \beta_{\text{TSPD}} &\leq \frac{1}{2h} \mathbb{E}[C_3] \\ &= \frac{1}{2h} \int_0^\infty \int_0^\infty \int_{[0,1]^3} e^{-z_1 - z_2} \max \left\{ \sqrt{(z_1 + z_2)^2 + h^4(u_0 - u_2)^2}, \right. \\ &\quad \left. \frac{1}{\alpha} \left(\sqrt{z_1^2 + h^4(u_0 - u_1)^2} + \sqrt{z_2^2 + h^4(u_1 - u_2)^2} \right) \right\} du dz_1 dz_2, \quad (6) \end{aligned}$$

where we used $u = (u_0, u_1, u_2)$ as a three-dimensional vector.

4.3 Quartet Rings Only

To extend our discussion to quartet rings and other more complicated cases, we define

$$W_i = \sum_{j=0}^i Z_j, \quad i = 0, 1, 2, \dots \quad (7)$$

$$W_0 = Z_0 = 0, \quad (8)$$

$$L_{ij} = \sqrt{(W_j - W_i)^2 + h^4(U_i - U_j)^2}, \quad i, j = 0, 1, 2, \dots \quad (9)$$

$$L_{ij} = L_{ji}. \quad (10)$$

We consider a quartet ring consists of $\{X_0, X_1, X_2, X_3\}$ and the unscaled distances of L_{01} , L_{12} , L_{23} , L_{02} , and L_{13} . While X_0 and X_3 are fixed as endpoints, we have options to choose either X_1 or X_2 as a drone node. In the decision making, we, of course, want to make C_4 as small as possible for a tighter upper bound. That is,

$$C_4 = \min \left\{ \max \left\{ L_{01} + L_{13}, \frac{1}{\alpha}(L_{02} + L_{03}) \right\}, \max \left\{ L_{02} + L_{23}, \frac{1}{\alpha}(L_{01} + L_{13}) \right\} \right\}.$$

The calculation of C_4 can be slightly simplified.

Lemma 3. We can show that

$$C_4 = \max \left\{ T_{\min}, \frac{1}{\alpha} T_{\max} \right\} \quad (11)$$

where $T_{\min} = \min\{L_{01} + L_{13}, L_{02} + L_{23}\}$ and $T_{\max} = \max\{L_{01} + L_{13}, L_{02} + L_{23}\}$.

Proof. Among $\{X_0, X_1, X_2, X_3\}$, X_0 and X_3 are fixed as the combined nodes. There are two possible cases: X_1 is the drone node, or X_2 . Comparing these two cases, we take the minimum. We can show that

$$\begin{aligned} C_4 &= \min \left\{ \max \left\{ L_{01} + L_{13}, \frac{1}{\alpha}(L_{02} + L_{23}) \right\}, \max \left\{ L_{02} + L_{23}, \frac{1}{\alpha}(L_{01} + L_{13}) \right\} \right\} \\ &= \max \left\{ \min\{L_{01} + L_{13}, L_{02} + L_{23}\}, \frac{1}{\alpha} \max\{L_{01} + L_{13}, L_{02} + L_{23}\} \right\}. \end{aligned}$$

This completes the proof. \square

Since we can determine T_{\min} and T_{\max} from the same comparison operation, Lemma 3 will help reduce computational effort slightly.

After forming a series of quartet rings within a strip, we may have one or two leftover points at the end, which we connect by straight rings. Again, such straight rings have a total length of $o(\sqrt{n})$ and therefore do not affect β_{TSPD} . Since each quartet ring, a 4-point ring, consumes 3 additional points, by using only quartet rings we can bound the limit as

$$\beta_{\text{TSPD}} \leq \frac{1}{3h} \mathbb{E}[C_4] = \frac{1}{3h} \int_0^\infty \int_0^\infty \int_0^\infty \int_{[0,1]^4} e^{-(z_1+z_2+z_3)} \max\{T_{\min}, \frac{1}{\alpha} T_{\max}\} du dz_1 dz_2 dz_3,$$

where we used $u = (u_0, u_1, u_2, u_3)$ as a vector.

4.4 General Cases of Homogeneous Ring Types

So far, we have considered 2-point rings (straight), 3-point rings (triangle), and 4-point rings (quartet). We can continue to consider 5-point rings, 6-point rings, etc. In general, with C_k for an integer $k \geq 2$, we can write

$$\beta_{\text{TSPD}}(\alpha) \leq \inf_{h>0} \frac{1}{(k-1)h} \mathbb{E}[C_k(h, \alpha)] \quad (12)$$

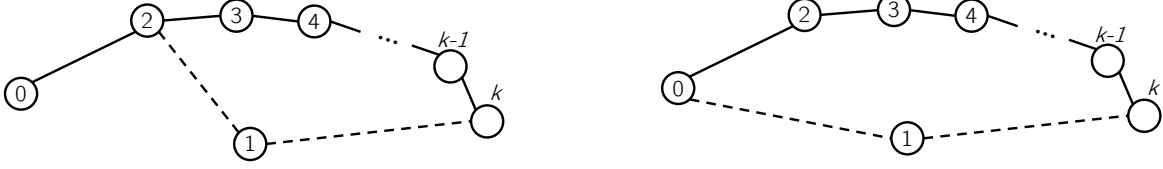


Figure 5: We can merge a straight ring to a neighboring ring to create a solution no worse than the current one.

for any given $\alpha \geq 1$. We can also write

$$\beta_{\text{TSPD}}(\alpha) \leq \min_{k \geq 2} \inf_{h > 0} \frac{1}{(k-1)h} \mathbb{E}[C_k(h, \alpha)].$$

However, considering many $k \geq 2$ values will be impractical for evaluating the bound, if not impossible. We limit our choice of k up to 2, 3, and 4, for homogeneous-ring formations as in Sections 4.1 to 4.3.

4.5 Alternating among k -point Ring Patterns

Instead of sticking to a single type of ring, we can also alternate among different types of rings. When $k = 2$ and $k = 3$, the only possibilities are a straight ring and a triangle ring, respectively, that are determined uniquely. We consider when $k \geq 4$.

Before we discuss alternating patterns, we make an important observation. It is known that there exists an optimal TSPD solution without two consecutive straight rings (Lee et al.; 2025). We strengthen this result.

Theorem 4. For any given TSPD, there exists an optimal solution without any straight rings.

Proof. Suppose there exists a straight ring as in the left figure of Figure 5, which is next to a k -point ring, wherein node 2 is the drone node. We show that

$$\begin{aligned} L_{02} + \max \left\{ L_{23} + \cdots + L_{k-1,k}, \frac{1}{\alpha} (L_{21} + L_{1k}) \right\} \\ \geq \max \left\{ L_{02} + L_{23} + \cdots + L_{k-1,k}, \frac{1}{\alpha} (L_{01} + L_{1k}) \right\} \end{aligned}$$

for any $\alpha \geq 1$, where the left-hand side represents the left figure and the right-hand side represents the right figure in Figure 5. From the triangle 012, we have $L_{01} \leq L_{02} + L_{21}$. With $\alpha \geq 1$, we obtain

$$\frac{1}{\alpha} (L_{01} + L_{1k}) \leq \frac{1}{\alpha} (L_{02} + L_{21} + L_{1k}) \leq \frac{1}{\alpha} (L_{21} + L_{1k}) + L_{02}.$$

Hence, we obtain

$$\begin{aligned} & L_{02} + \max \left\{ L_{23} + \cdots + L_{k-1,k}, \frac{1}{\alpha} (L_{21} + L_{1k}) \right\} \\ &= \max \left\{ L_{02} + L_{23} + \cdots + L_{k-1,k}, L_{02} + \frac{1}{\alpha} (L_{21} + L_{1k}) \right\} \\ &\geq \max \left\{ L_{02} + L_{23} + \cdots + L_{k-1,k}, \frac{1}{\alpha} (L_{01} + L_{1k}) \right\}, \end{aligned}$$

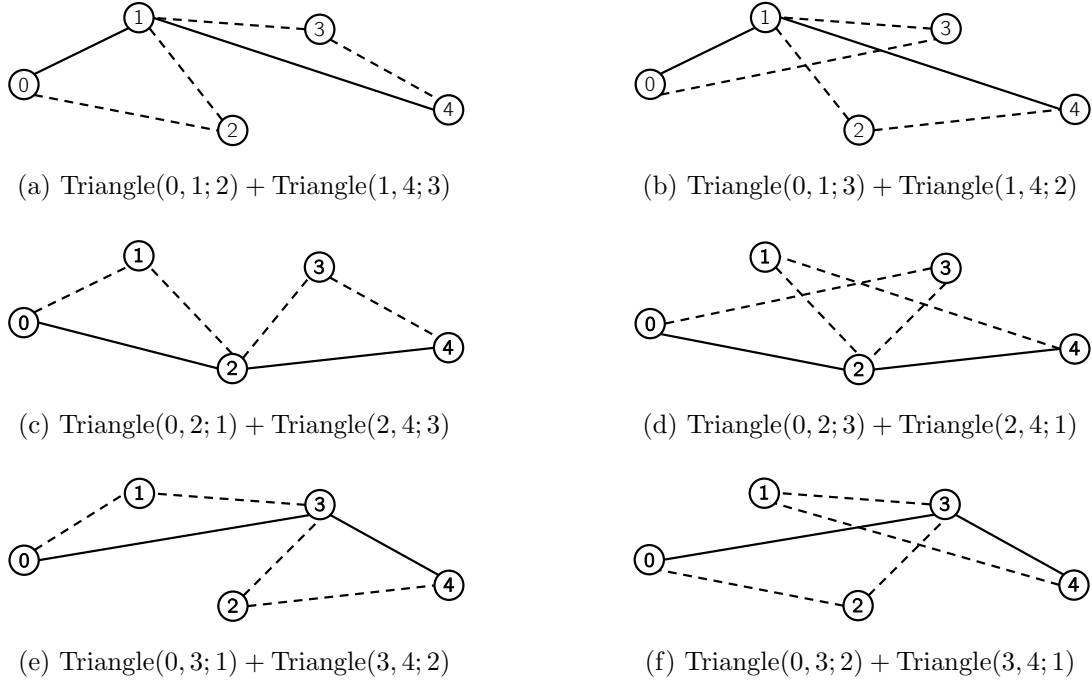


Figure 6: Triangle-Triangle patterns with five points. Note that only the ordering of the horizontal coordinates is important in this figure; therefore, the shape shown in the figure may not represent the actual distance.

which shows that you can merge a straight ring to a neighboring ring without increasing the total cost. \square

This theorem will help us simplify the calculations.

4.5.1 Four-point Ring Patterns

We assume that we consider a block of 4 points each time, and determine the best choice of ring composition. There are three cases: (i) Triangle-Straight, (ii) Straight-Triangle, and (iii) Quartet. Theorem 4, however, tells that Triangle-Straight and Straight-Triangle patterns are no better than the Quartet patterns. That is, by merging the straight ring with the neighboring triangle ring, we obtain a quartet ring without increasing the objective function value. Therefore, for four-point ring patterns, we only need to consider quartet rings as done in Section 4.3.

4.5.2 Five-point Ring Patterns

We now consider a block of 5 points each time. We consider the following five cases: (i) Triangle-Triangle, (ii) Quartet-Straight, (iii) Straight-Quartet, (iv) Straight-Triangle-Straight, and (v) Quintets. Again, by Theorem 4, we can merge all straight rings in cases (ii), (iii), and (iv), to obtain a quintet ring. Therefore, we only consider the Triangle-Triangle patterns, presented in Figure 6, and the Quintet patterns, presented in Figure 7.

There are 12 total possibilities. Similar to the previous discussion, we define L_{01} , L_{12} , L_{23} ,

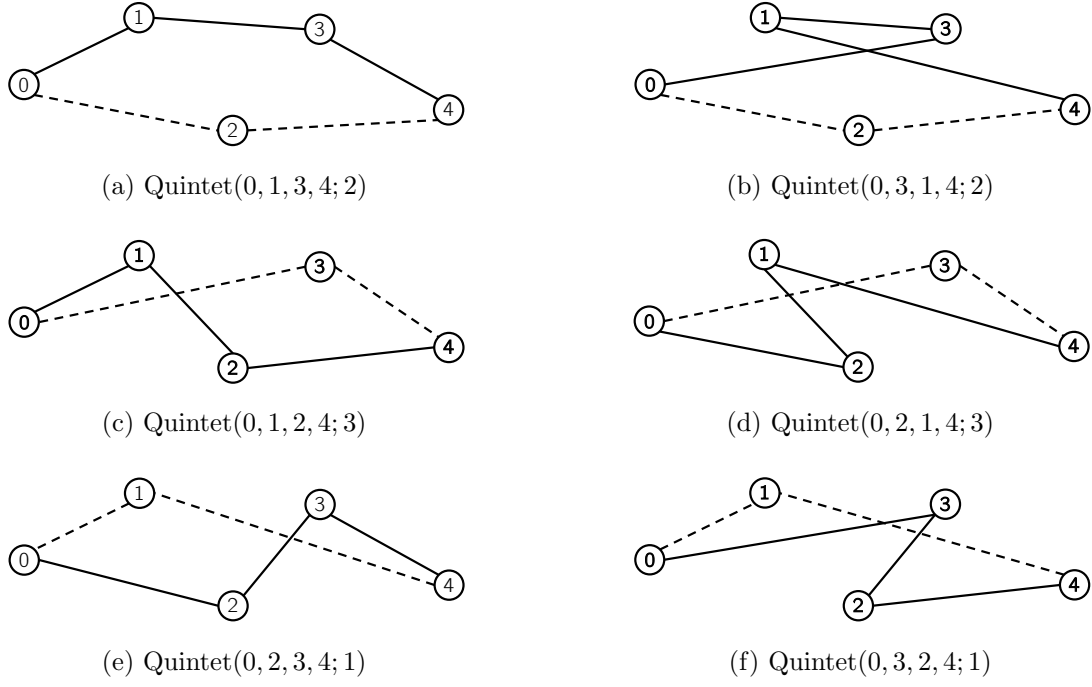


Figure 7: Quintet patterns. Note that only the ordering of the horizontal coordinates is important in this figure; therefore, the shape shown in the figure may not represent the actual distance.

L_{34} , L_{02} , L_{03} , L_{13} , and L_{14} using (7)–(10). Let us define the following shorthands:

$$\text{Triangle}(i, j; k) = \max \left\{ L_{ij}, \frac{1}{\alpha} (L_{ik} + L_{kj}) \right\}$$

to represent the triangle ring where the truck travels from node i to node j and the drone visits node k , and

$$\text{Quintet}(i, i_1, i_2, j; k) = \max \left\{ L_{ii_1} + L_{i_1i_2} + L_{i_2j}, \frac{1}{\alpha} (L_{ik} + L_{kj}) \right\}$$

to represent the quintet ring where the truck travels from node i to i_1 to i_2 to j and the drone visits node k .

After considering all 12 possibilities, we take the minimum and multiply it by $\frac{1}{4h}$ to obtain the following lower bound:

$$\frac{1}{4h} \mathbb{E} \left[\min \left\{ \begin{aligned} &\text{Triangle}(0, 1; 2) + \text{Triangle}(1, 4; 3), \quad \text{Triangle}(0, 1; 3) + \text{Triangle}(1, 4; 2), \\ &\text{Triangle}(0, 2; 1) + \text{Triangle}(2, 4; 3), \quad \text{Triangle}(0, 2; 3) + \text{Triangle}(2, 4; 1), \\ &\text{Triangle}(0, 3; 1) + \text{Triangle}(3, 4; 2), \quad \text{Triangle}(0, 3; 2) + \text{Triangle}(3, 4; 1), \\ &\text{Quintet}(0, 1, 3, 4; 2), \quad \text{Quintet}(0, 3, 1, 4; 2), \quad \text{Quintet}(0, 1, 2, 4; 3), \\ &\text{Quintet}(0, 2, 1, 4; 3), \quad \text{Quintet}(0, 2, 3, 4; 1), \quad \text{Quintet}(0, 3, 2, 4; 1) \end{aligned} \right\} \right].$$

The evaluation of the above bound requires 9-dimensional numerical integration. For such multi-dimensional integration, Monte Carlo or quasi-Monte Carlo methods are widely used, since

the standard quadrature-based methods suffer from the curse of dimensionality (Cafisch; 1998).

5 Lower Bounds

Considering the speed-scaled Euclidean distance model in Section 3.3, we turn our attention to lower bounds of β_{TSPD} . We first notice this result:

Lemma 4 (Agatz et al. 2018). For any given points x_1, \dots, x_n , it holds that

$$\frac{1}{1+\alpha} \text{TSP}(\{x_1, \dots, x_n\}) \leq \text{TSPD}(\{x_1, \dots, x_n\}) \quad (13)$$

for any $\alpha \geq 1$.

This lemma immediately gives that

$$\beta_{\text{TSPD}} \geq \frac{\beta_{\text{TSP}}}{1+\alpha} \geq \frac{\beta}{1+\alpha} \quad (14)$$

for any lower bound β for β_{TSP} . When $\beta = 0.6277$ and $\alpha = 2$, we obtain

$$\beta_{\text{TSPD}} \geq 0.2092.$$

While this is a valid bound, it does not consider any large-scale behavior. We are interested in a tighter bound for β_{TSPD} .

Consider n points, X_1, \dots, X_n , uniformly distributed on $[0, 1]^2$, and suppose that a TSPD solution is given. Let n_T be the number of nodes visited by the truck—truck nodes and combined nodes—and n_D be the number of drone nodes. Let the total distance traveled by the truck be L_T and the total distance traveled by the drone *alone* be L_D . We let L be the makespan of the TSPD. We dropped the function argument for brevity; for example $L = \text{TSPD}(\{X_1, \dots, X_n\})$.

For any given TSPD solution and given split of node numbers (n_T, n_D) , we have

$$L \geq \max \left\{ L_T, \frac{1}{\alpha} L_D \right\}.$$

Therefore, by taking the expectations, we obtain

$$\mathbb{E}L \geq \mathbb{E} \max \left\{ L_T, \frac{1}{\alpha} L_D \right\} \geq \max \left\{ \mathbb{E}L_T, \frac{1}{\alpha} \mathbb{E}L_D \right\}.$$

Considering a constant $\rho \in (0, 1]$, we let $n_T = \rho n$ and $n_D = (1 - \rho)n$. We have

$$\mathbb{E}L \geq \inf_{\rho \in (0, 1]} \max \left\{ \mathbb{E}L_T, \frac{1}{\alpha} \mathbb{E}L_D \right\}. \quad (15)$$

Using this, we present the following result:

Theorem 5. Let β be a lower bound for β_{TSP} . Then the following holds:

$$\beta_{\text{TSPD}} \geq \beta \sqrt{\frac{5}{5 + 4\alpha\beta}}, \quad (16)$$

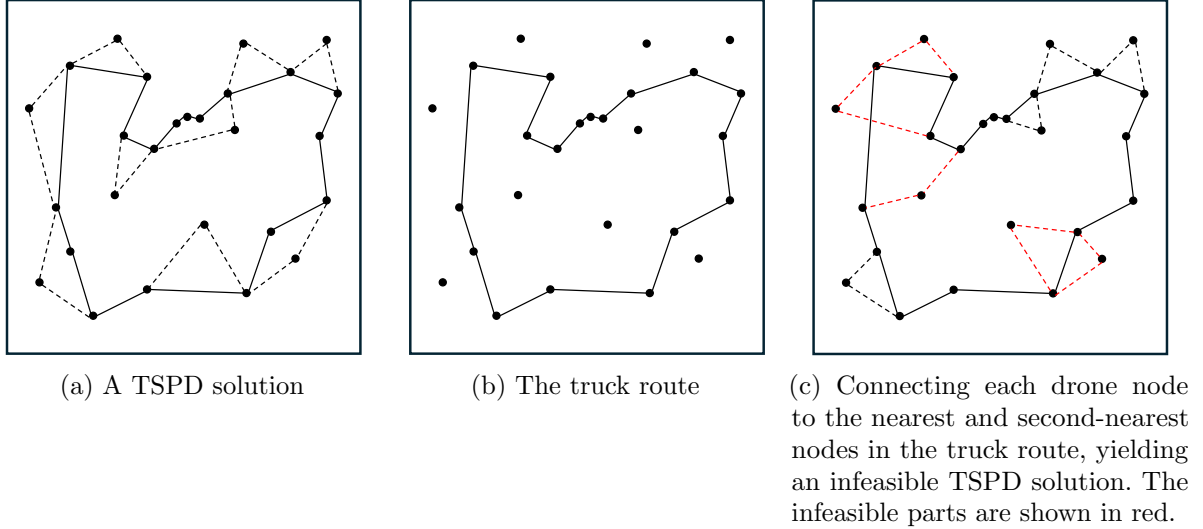


Figure 8: Constructing a lower bound

for any $\alpha \geq 1$.

Proof. While there is no guarantee that the truck route follows an optimal TSP tour in an optimal TSPD solution, the length of the truck route is certainly bounded below by the length of the TSP tour passing n_T points. Therefore, we have

$$\mathbb{E}L_T \geq \beta_{\text{TSP}}\sqrt{n_T}, \quad (17)$$

when n_T is sufficiently large. Note that (17) is also valid for any lower bound β for β_{TSP} .

We now consider a lower bound for $\mathbb{E}L_D$, following the procedure illustrated in Figure 8. Given a feasible TSPD solution, we remove all drone arcs. Then, each drone node is connected to the nearest and second-nearest points among the points visited by the truck. Such connections may not yield a feasible TSPD solution, but they do yield a lower bound on L_D . By Lemma 2, the expected length of these two connections is given by

$$\left(\frac{1}{2} + \frac{3}{4}\right) \frac{1}{\sqrt{n_T}} = \frac{5}{4} \frac{1}{\sqrt{n_T}}, \quad (18)$$

which yields

$$\mathbb{E}L_D \geq \frac{5}{4} \frac{n_D}{\sqrt{n_T}}.$$

Combining the two bounds, we have

$$\mathbb{E}L \geq \max \left\{ \beta\sqrt{n_T}, \frac{5}{4\alpha} \frac{n_D}{\sqrt{n_T}} \right\}.$$

Letting $n_T = \rho n$ and $n_D = (1 - \rho)n$, we obtain the following parametric bound:

$$\frac{\mathbb{E}L}{\sqrt{n}} \geq \max \left\{ \beta\sqrt{\rho}, \frac{5}{4\alpha} \frac{1 - \rho}{\sqrt{\rho}} \right\}.$$

Since we do not know the true value of ρ in an optimal TSPD solution, we minimize the

Table 1: Numerical results for the speed-scaled Euclidean TSPD model. (1) The top section presents the Monte Carlo evaluation of the upper bounds on β_{TSPD} with 20 million samples. (2) The middle section presents values obtained by the heuristic solutions of TSPD; the average of 100 random instances is reported for each (n, α) . (3) The bottom section presents the lower bounds calculated with a lower bound β for β_{TSP} ; note that $\beta = 0.6277$ is a valid lower bound of β_{TSP} , while $\beta = 0.71$ is an empirically guessed value of β_{TSP} .

		TSPD/ \sqrt{n}				
		$\alpha = 1.0$	$\alpha = 1.5$	$\alpha = 2.0$	$\alpha = 2.5$	$\alpha = 3.0$
n	straight only	0.9212	0.9212	0.9212	0.9212	0.9212
	triangle only	0.9211	0.7423	0.6905	0.6670	0.6548
	quartet only	0.8316	0.6838	0.6567	0.6483	0.6451
	5-point patterns	0.7605	0.6544	0.6130	0.5828	0.5615
	20	0.6924	0.6084	0.5640	0.5346	0.5158
	30	0.6812	0.6019	0.5571	0.5305	0.5105
	50	0.6603	0.5821	0.5413	0.5128	0.4931
	75	0.6383	0.5637	0.5243	0.4977	0.4781
	100	0.6344	0.5607	0.5223	0.4977	0.4803
	200	0.6206	0.5499	0.5132	0.4893	0.4725
β	500	0.6084	0.5397	0.5043	0.4818	0.4655
	1000	0.6021	0.5342	0.4993	0.4770	0.4609
	2000	0.5982	0.5316	0.4974	0.4756	0.4600
	5000	0.5946	0.5285	0.4946	0.4731	0.4576
	10000	0.5934	0.5277	0.4940	0.4726	0.4573
	0.71	0.5670	0.5217	0.4858	0.4564	0.4317
	0.6277	0.5121	0.4740	0.4433	0.4179	0.3964

right-hand side with respect to the parameter ρ to obtain a valid lower bound. The minimum occurs when the two terms in the max operator are equal. That is when

$$\rho = \frac{5}{5 + 4\alpha\beta},$$

which yields the lower bound in (16). Since the choice of ρ does not depend on n , we can ensure that n_T and n_D are sufficiently large whenever n is sufficiently large. This completes the proof. \square

6 Numerical Results

While the computation of a lower bound is immediate by (16), the upper bounds require evaluations of multi-dimensional integrals. Since these integrals represent expectations, Monte Carlo integration is a natural choice for numerical integration. See Robert et al. (1999), for example, for the details of Monte Carlo integration. We implemented a classical Monte Carlo integration in the Julia language and used the `Optim.jl` package (Mogensen and Riseth; 2018) to find the best h value for each simulation.

Table 1 reports the computational results for the speed-scaled Euclidean TSPD model. The

top section displays the upper bound values obtained via Monte Carlo integration for various ring patterns; these values are averaged and then rounded. As anticipated, the 5-point patterns provide the best bounds, while the bounds improve as we use more complicated ring patterns. The bottom section lists the lower-bound values computed from β . We tested two values, $\beta = 0.6277$ as a lower bound for β_{TSP} and $\beta = 0.71$ as an empirical value of β_{TSP} . These lower-bound values are truncated.

To compare the upper and lower bounds for TSPD, we obtained actual solutions of TSPD in the middle section of Table 1. Since we do not have an exact algorithm for large-scale TSPD, we used the iterative chainlet partitioning (ICP) algorithm of Lee et al. (2025) to obtain high-quality heuristic solutions. The ICP algorithm starts with an initial TSP tour and iteratively improves it via local search and dynamic programming. Compared to existing algorithms, ICP provides the best solutions for most benchmark instances. We obtained initial tours by the LKH solver (Helsgaun; 2000). We solved 100 randomly generated instances for each instance size n and reported the average value, rounded to 4 decimal places. Since ICP is a heuristic algorithm, the values in Table 1 are approximations to upper bounds. By comparing the ICP solutions with the lower bounds, we reconfirm that ICP indeed produces high-quality solutions.

For $\alpha = 2.0$, we note that our upper and lower bounds were 0.6130 and 0.4433, while the empirical value by ICP is 0.493986. When we used the empirical TSP limit $\beta_{\text{TSP}} = 0.71$, our lower bound for TSPD was 0.485800, which is quite close to the empirical value. Given this evidence, we conjecture that $\beta_{\text{TSPD}} \approx 0.49$ for $\alpha = 2.0$.

7 The Rectilinear-Euclidean Mixed TSPD Model

It is possible to extend our result to the Rectilinear-Euclidean mixed model in Section 3.4. Although an upper bound can be obtained with some modifications, we omit the discussion. In this section, we make simple observations on the lower bound.

We first obtain a lower bound for the TSP with ℓ_1 -norm. Let $A(r)$ denote the area of the metric ball with radius r . For the ℓ_1 -norm, $A(r) = 2r^2$, and for the ℓ_2 -norm, $A(r) = \pi r^2$. Lemma 2 treated the ℓ_2 -norm case. Following the treatment of Mathai (1999, Section 2.4.1), we can easily obtain a similar result for the ℓ_1 -norm:

Lemma 5. Let \mathcal{P}_n be a Poisson process on \mathbb{R}^2 with intensity n , and the distances are measured using the ℓ_1 -norm. Then, for any fixed point $p \in \mathbb{R}^2$, the probability density of the distance between p and the nearest point in \mathcal{P}_n is given by $f_1(r) = 4nre^{-2nr^2}$ and its expectation is $\frac{\sqrt{2\pi}}{4\sqrt{n}}$. The distance to the second-nearest point is distributed by $f_2(r) = 8n^2r^3e^{-2nr^2}$ and its expectation is $\frac{3\sqrt{2\pi}}{8\sqrt{n}}$.

Using the same argument as in Section 5, we can use Lemma 5 for a lower bound for the optimal TSP tour length with ℓ_1 -norm:

$$\left(\frac{\sqrt{2\pi}}{4} + \frac{3\sqrt{2\pi}}{8} \right) \frac{1}{\sqrt{n}} \frac{n}{2} = \frac{5\sqrt{2\pi}}{16} \sqrt{n} > 0.7833\sqrt{n}.$$

Note that this lower bound may be improved by the techniques used in Steinerberger (2015) and Gaudio and Jaillet (2020), which are outside the scope of this paper.

Table 2: Rectilinear TSP tour costs (truck-only baseline) obtained by the LKH solver. The average of 100 random instances is reported for each n .

n	TSP	TSP/ \sqrt{n}
20	4.7285	1.0573
30	5.7170	1.0438
50	7.0755	1.0006
75	8.4521	0.9762
100	9.6791	0.9679
200	13.3637	0.9449
500	20.6956	0.9255
1000	28.9670	0.9159
2000	40.6885	0.9097
5000	63.8350	0.9028
10000	90.1056	0.9011

Table 3: Numerical results for the Rectilinear-Euclidean Mixed TSPD model. (1) The first section presents values obtained by the heuristic solutions of TSPD; the average of 100 random instances is reported for each (n, α) . (2) The second section presents the lower bounds calculated with a lower bound β for β_{TSP} ; note that $\beta = 0.783321$ is a valid lower bound of β_{TSP} , while $\beta = 0.90$ is an empirical value of β_{TSP} guessed from Table 2.

		TSPD/ \sqrt{n}				
		$\alpha = 1.0$	$\alpha = 1.5$	$\alpha = 2.0$	$\alpha = 2.5$	$\alpha = 3.0$
n	20	0.7962	0.7099	0.6690	0.6414	0.6140
	30	0.7967	0.7167	0.6687	0.6363	0.6019
	50	0.7845	0.7054	0.6549	0.6184	0.5943
	75	0.7691	0.6892	0.6403	0.6038	0.5771
	100	0.7754	0.7005	0.6523	0.6126	0.5861
	200	0.7736	0.7010	0.6489	0.6100	0.5795
	500	0.7564	0.6916	0.6440	0.6086	0.5818
	1000	0.7540	0.6892	0.6426	0.6072	0.5797
	2000	0.7533	0.6882	0.6415	0.6064	0.5795
	5000	0.7493	0.6848	0.6386	0.6043	0.5778
10000	0.7038	0.6437	0.6004	0.5683	0.5438	
β	0.90	0.6862	0.6240	0.5761	0.5378	0.5062
	0.7833	0.6147	0.5623	0.5218	0.4889	0.4615

In Theorem 5, by letting $\beta = 0.7833$ and $\alpha = 2.0$, we obtain a lower bound for the Rectilinear-Euclidean mixed TSPD model as follows:

$$\beta_{\text{TSPD}} \geq \beta \sqrt{\frac{5}{5 + 4\alpha\beta}} > 0.5218.$$

When the truck distance is rectilinear, the LKH solutions seem to converge to 0.90, as shown in Table 2. When we use this empirical value of $\beta = 0.90$, the above lower bound becomes 0.5761. Since LKH solutions are not guaranteed to be optimal, this value is provided only for reference. For other values of α , lower bounds are provided in the bottom section of Table 3.

The top section of Table 3 presents the empirical limit calculated by the ICP algorithm, which is close to 0.6004 when $\alpha = 2.0$ and $n = 10000$. Unlike the Euclidean case, however, the ICP solutions for the Rectilinear-Euclidean mixed model exhibit slower convergence rates as n increases. This suggests that the mixed-norm TSPD requires larger n to stabilize than the pure Euclidean case. Consequently, while the current empirical value is around 0.60 when $n = 10,000$, the true asymptotic constant is likely lower, potentially closer to 0.58.

8 Concluding Remarks

We established a Beardwood–Halton–Hammersley-type asymptotic limit for the Traveling Salesman Problem with Drone (TSPD). Our analysis combines subadditive Euclidean functional arguments with structured ring-based tour constructions to derive upper and lower bounds for the speed-scaled Euclidean TSPD model. A key insight is that optimal TSPD solutions can be assumed to exclude truck-drone co-travel segments, which significantly reduces the computational burden and enables efficient Monte Carlo evaluations. We also developed a parametric lower-bound framework that links cooperative routing to classical TSP asymptotics and nearest-neighbor distance distributions. The proposed methodological framework would provide a general template for analyzing the asymptotic behavior of a broader class of cooperative and multi-modal routing problems with synchronization constraints and heterogeneous distance metrics.

Numerical experiments demonstrate that the proposed bounds are tight. For the speed-scaled Euclidean model, our results suggest that the TSPD constant is close to 0.49 when the drone travels twice as fast as the truck. For practical strategic planning, this result supports the use of the following continuous approximation formula for the optimal TSPD makespan serving n customers in a service region of area A : $\text{TSPD} \approx 0.49\sqrt{nA}$.

Acknowledgements

This work was supported by the National Research Foundation of Korea (NRF) grant funded by the Korean government (MSIT) (RS-2023-00259550).

References

- Agatz, N., Bouman, P. and Schmidt, M. (2018). Optimization Approaches for the Traveling Salesman Problem with Drone, *Transportation Science* **52**(4): 965–981.
- Ansari, S., Başdere, M., Li, X., Ouyang, Y. and Smilowitz, K. (2018). Advancements in continuous approximation models for logistics and transportation systems: 1996–2016, *Transportation Research Part B: Methodological* **107**: 229–252.
- Arslan, O. (2021). The location-or-routing problem, *Transportation Research Part B: Methodological* **147**: 1–21.
- Banerjee, D., Erera, A. L., Stroh, A. M. and Toriello, A. (2023). Who has access to e-commerce and when? time-varying service regions in same-day delivery, *Transportation Research Part B: Methodological* **170**: 148–168.
- Beardwood, J., Halton, J. H. and Hammersley, J. M. (1959). The shortest path through many points, *Mathematical Proceedings of the Cambridge Philosophical Society* **55**(4): 299–327.
- Bogyrbayeva, A., Yoon, T., Ko, H., Lim, S., Yun, H. and Kwon, C. (2023). A deep reinforcement learning approach for solving the traveling salesman problem with drone, *Transportation Research Part C: Emerging Technologies* **148**: 103981.
- Caffisch, R. E. (1998). Monte Carlo and quasi-Monte Carlo methods, *Acta Numerica* **7**: 1–49.
- Carlsson, J. G. and Jones, B. (2022). Continuous approximation formulas for location problems, *Networks* **80**(4): 407–430.
- Carlsson, J. G. and Song, S. (2018). Coordinated logistics with a truck and a drone, *Management Science* **64**(9): 4052–4069.
- Carlsson, J. G. and Yu, J. (2025). A new upper bound for the Euclidean TSP constant, *INFORMS Journal on Computing* .
- Choi, Y. and Schonfeld, P. M. (2022). Review of length approximations for tours with few stops, *Transportation Research Record* **2676**(3): 201–213.
- Daganzo, C. F. (1984a). The distance traveled to visit n points with a maximum of c stops per vehicle: An analytic model and an application, *Transportation Science* **18**(4): 331–350.
- Daganzo, C. F. (1984b). The length of tours in zones of different shapes, *Transportation Research Part B: Methodological* **18**(2): 135–145.
- de Freitas, J. C. and Penna, P. H. V. (2020). A variable neighborhood search for flying sidekick traveling salesman problem, *International Transactions in Operational Research* **27**(1): 267–290.
- Fu, C., Ma, S., Zhu, N., He, Q.-C. and Yang, H. (2022). Bike-sharing inventory management for market expansion, *Transportation Research Part B: Methodological* **162**: 28–54.

- Gaudio, J. and Jaillet, P. (2020). An improved lower bound for the traveling salesman constant, *Operations Research Letters* **48**(1): 67–70.
- Helsgaun, K. (2000). An effective implementation of the Lin-Kernighan traveling salesman heuristic, *European Journal of Operational Research* **126**(1): 106–130.
- Johnson, D. S., McGeoch, L. A. and Rothberg, E. E. (1996). Asymptotic experimental analysis for the Held-Karp traveling salesman bound, *Proceedings of the 7th Annual ACM-SIAM Symposium on Discrete Algorithms*, Vol. 341, ACM press San Francisco, p. 350.
- Langevin, A., Mbaraga, P. and Campbell, J. F. (1996). Continuous approximation models in freight distribution: An overview, *Transportation Research Part B: Methodological* **30**(3): 163–188.
- Lee, J. H., Kim, M., Kim, M., Park, J. and Kwon, C. (2025). The iterative chainlet partitioning algorithm for the traveling salesman problem with drone and neural acceleration, *arXiv preprint arXiv:2504.15147*.
- Mahmoudinazlou, S. and Kwon, C. (2024). A hybrid genetic algorithm with type-aware chromosomes for traveling salesman problems with drone, *European Journal of Operational Research* **318**(3): 719–739.
- Mathai, A. M. (1999). *An Introduction to Geometrical Probability: Distributional Aspects with Applications*, Vol. 1, CRC Press.
- Mogensen, P. K. and Riseth, A. N. (2018). Optim: A mathematical optimization package for Julia, *Journal of Open Source Software* **3**(24): 615.
- Murray, C. C. and Chu, A. G. (2015). The flying sidekick traveling salesman problem: Optimization of drone-assisted parcel delivery, *Transportation Research Part C: Emerging Technologies* **54**: 86–109.
- Osorio, J., Lei, C. and Ouyang, Y. (2021). Optimal rebalancing and on-board charging of shared electric scooters, *Transportation Research Part B: Methodological* **147**: 197–219.
- Poikonen, S., Golden, B. and Wasil, E. A. (2019). A branch-and-bound approach to the traveling salesman problem with a drone, *INFORMS Journal on Computing* **31**(2): 335–346.
- Rhee, W. T. (1993). On the stochastic Euclidean travelling salesperson problem for distributions with unbounded support, *Mathematics of Operations Research* **18**(2): 292–299.
- Robert, C. P., Casella, G. and Casella, G. (1999). *Monte Carlo statistical methods*, Vol. 2, Springer.
- Steele, J. M. (1981). Subadditive Euclidean functionals and nonlinear growth in geometric probability, *The Annals of Probability* pp. 365–376.
- Steinerberger, S. (2015). New bounds for the traveling salesman constant, *Advances in Applied Probability* **47**(1): 27–36.
- Yukich, J. E. (2006). *Probability Theory of Classical Euclidean Optimization Problems*, Springer.